Mechanisms of membrane protein crystallization in "bicelles"

Tatiana N. Murugova, Oleksandr I. Ivankov, Yury L. Ryzhykau, Dmytro V. Soloviov, Kirill V. Kovalev, Daria V. Skachkova, Adam Round, Christian Baeken, Andrii V. Ishchenko, Oleksandr A. Volkov, Andrey V. Rogachev, Alexey V. Vlasov, Alexander I. Kuklin, Valentin I. Gordeliy

Why do we need protein crystals?

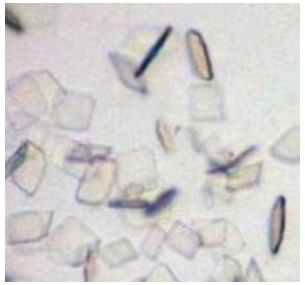

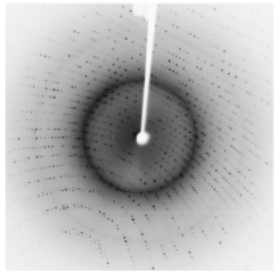

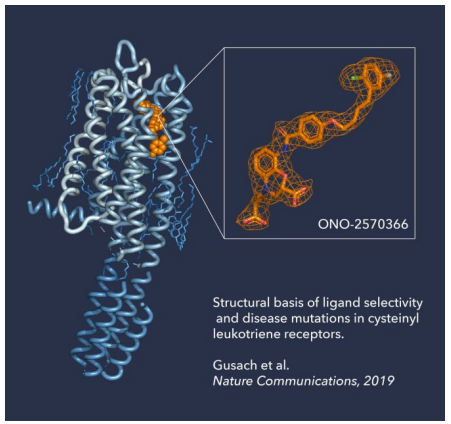

X-ray/neutron protein crystallography

1. Understanding the mechanisms of functioning of living systems at the protein level
2. Developing drugs (Rational design)
3. Proteins – the main target for drug design

How to grow protein crystals?

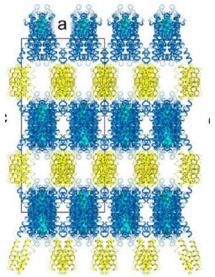

1. Trial and error method
2. Screening 100-1000s conditions
3. Time- and material-consumable
4. The result is not guaranteed

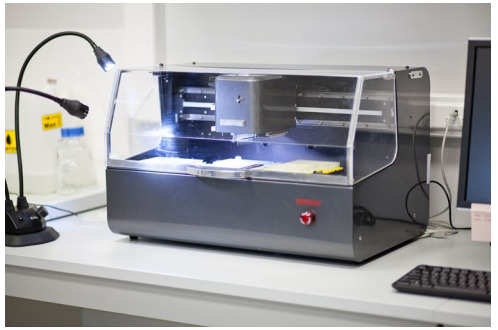

Fast nanoliter-volume liquid handler

Automated imaging system for protein crystallization

Gusach, A., Luginina, et al. Nat Commun 10, 5573 (2019).

Kermani AA. FEBS J. 2021 Oct;288(20):5788-5804.

The Research Center for Molecular Mechanisms of Aging and Age-Related Diseases at MIPT, Dolgoprudny. https://cmm-mipt.ru/high-throughput-protein-crystallization-platform.html

Membrane proteins

In vivo

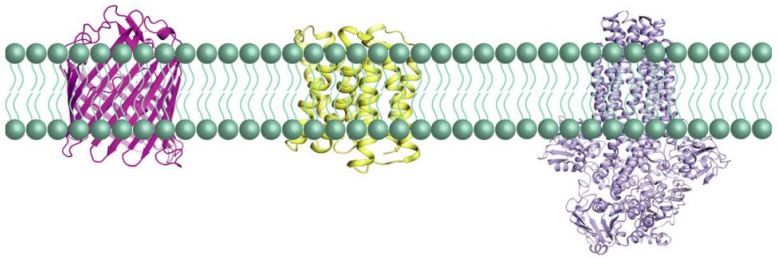

In vitro

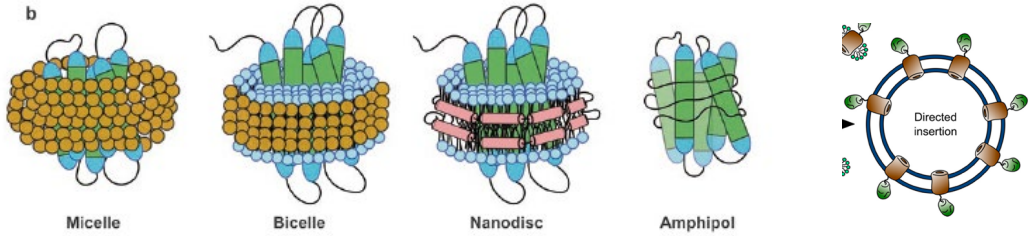

Kermani AA. A guide to membrane protein X-ray crystallography. FEBS J. 2021 Oct;288(20):5788-5804.

Ishchenko, A. et al. (2017) Protein Crystallography. Methods in Molecular Biology, vol 1607.

- Transport (ions, metabolites and large molecules such as proteins and RNA across their membranes)
- Energy conversion
- Signal transduction (chemical, photo signals, electrical impulses)
- Controlling membrane lipid composition
- Organization and maintain the shape of organelles and the cell itself
- 1/3 of the human genome encodes membrane proteins.
- Membrane proteins are the targets of about 60% of currently used drugs.

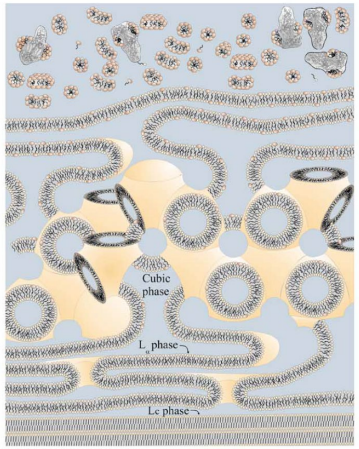

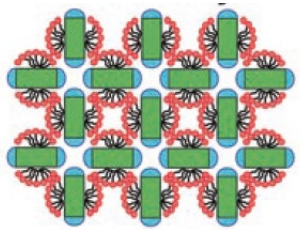

Caffrey M. Membrane protein crystallization. J Struct Biol. 2003 Apr;142(1):108-32

The aim of our study

- To monitor the evolution of structure of lipidic matrix during process of crystallization.
- To find out which structures the matrix adopts.
- What structural features are common for different approaches of crystallization of membrane proteins.
- Thus, to see important details and necessary steps facilitating the successful crystallization and how it can be used.

  for rational, thoughtful and controlled crystallization process.

Experimental details

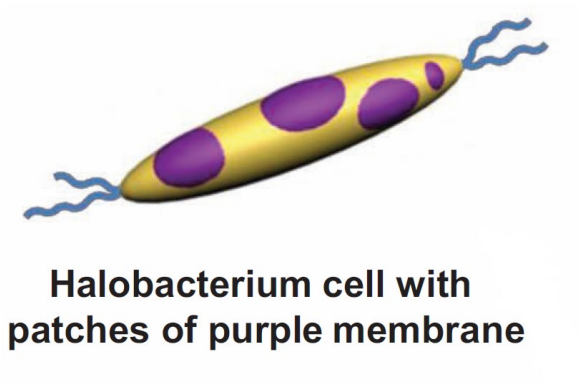

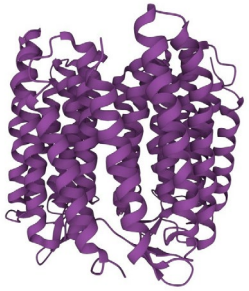

Bacteriorhodopsin (bR)
Light-driven proton pump

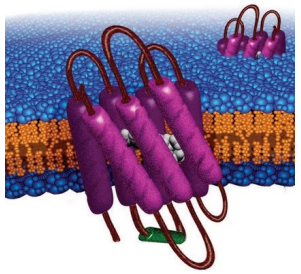

Purple membrane

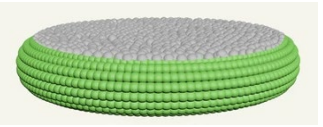

bicelles

Halobacterium salinarum in its natural environment – hypersaline surroundings. The picture shows a salty pond in the Arabian desert, which is colored red due to the presence of *H. salinarum.*

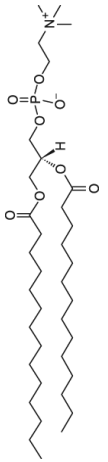

DMPC

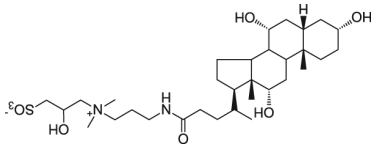

CHAPSO

G. de Q. Silveira, Z. Chen, E. F. Barry, B. T. Diroll, B. Lee, T. Rajh, E. A. Rozhkova, P. D. Laible, H. C. Fry, Energy Transfer Induced by Dye Encapsulation in a Hybrid Nanoparticle-Purple Membrane Reversible Assembly. *Adv. Funct. Mater.* 2019, 29, 1904899. https://doi.org/10.1002/adfm.201904899

Setup of experimental system

Typical

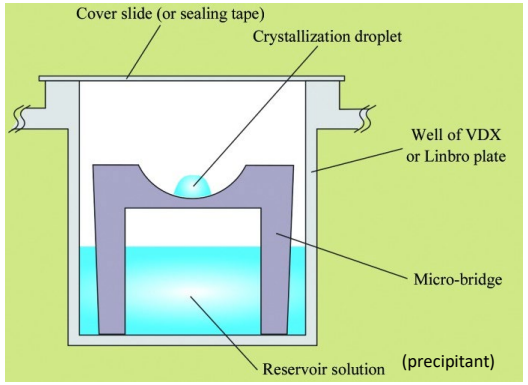

Adopted from McPherson A, Gavira JA. Acta Crystallogr F Struct Biol Commun. 2014 Jan;70(Pt 1):2-20.

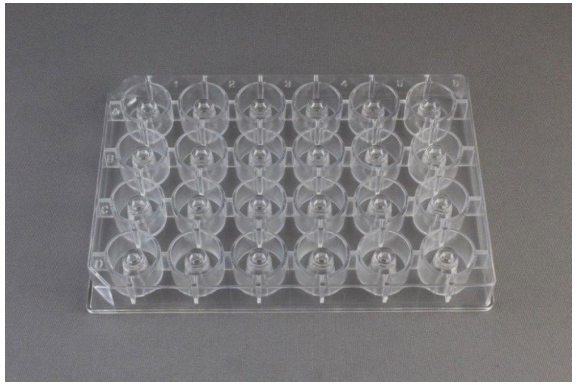

Crystallization plate
https://hamptonresearch.com

For SAXS

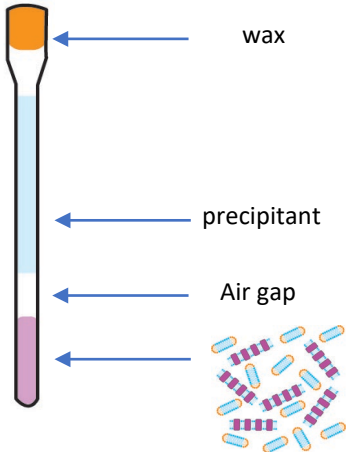

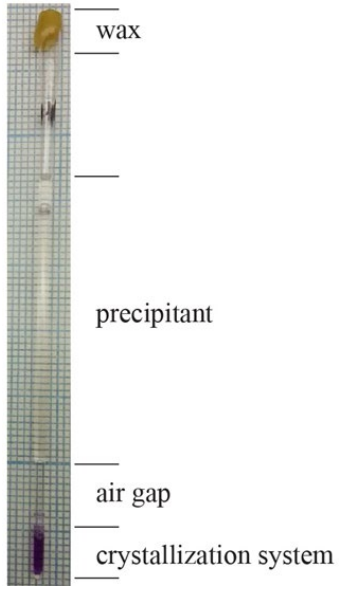

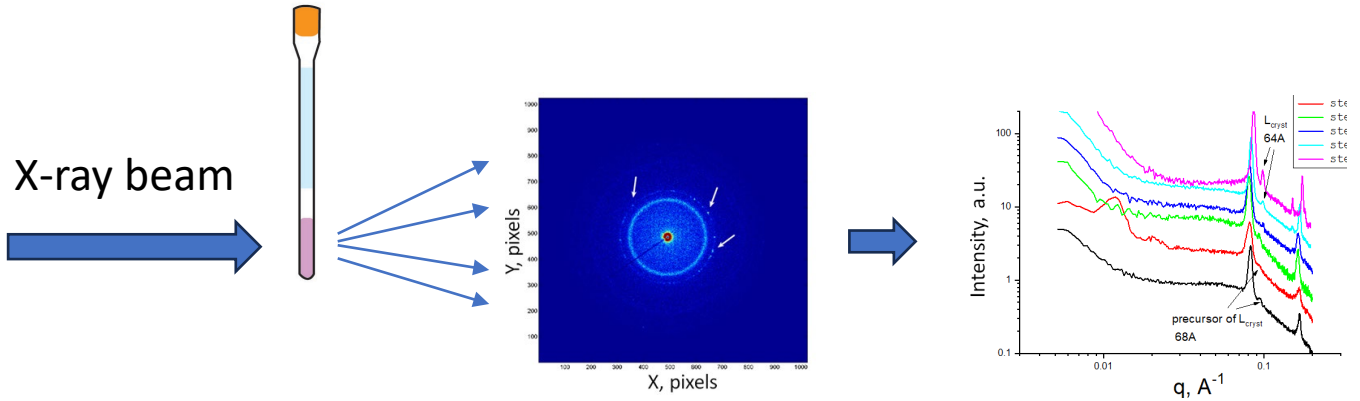

Real-time monitoring of structure evolution

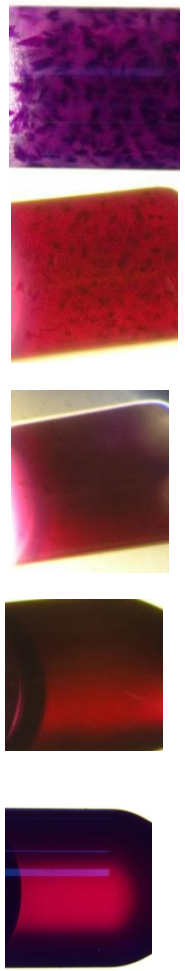

time

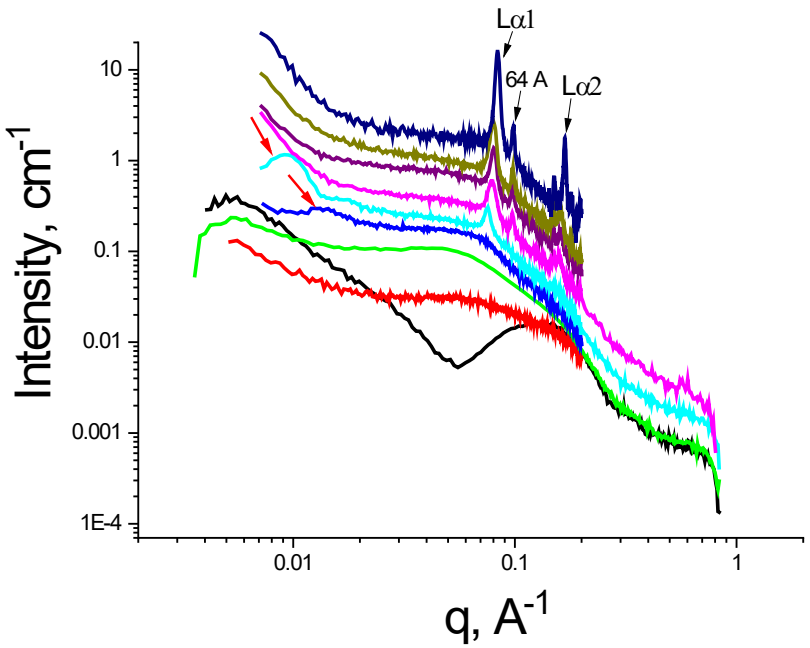

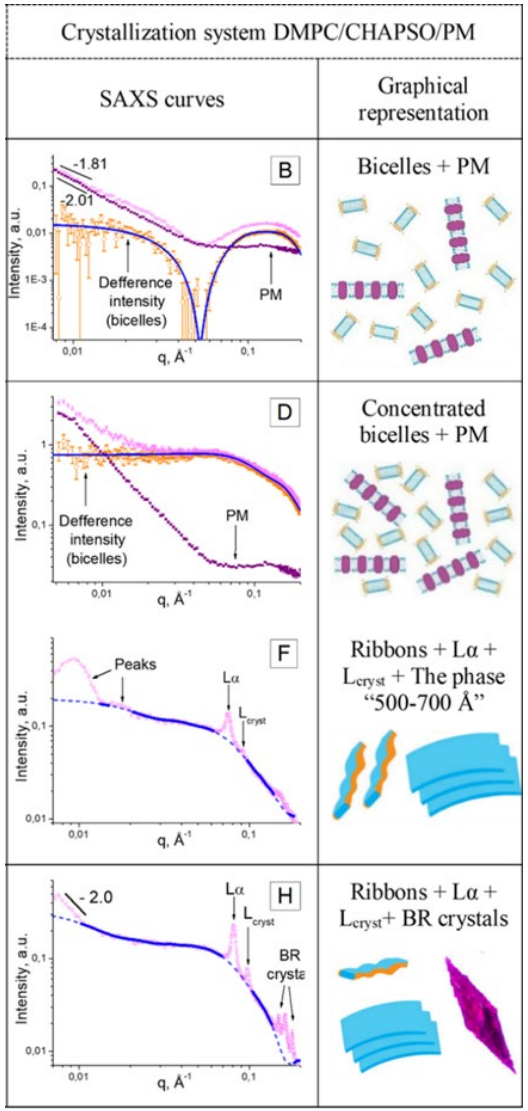

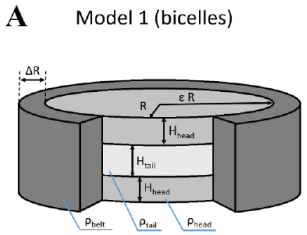

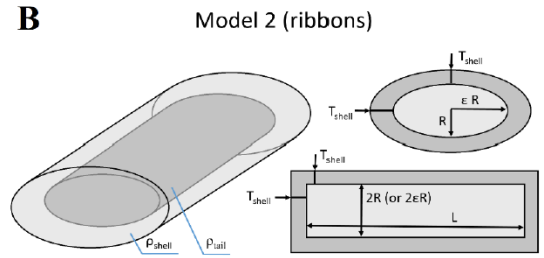

$$P(q) = \int_0^{\pi} d\theta \int_0^{2\pi} |F(q,\theta,\varphi)|^2 d\varphi \quad [5]$$

where

$$F(q,\theta,\varphi) = (\rho_{tail} - \rho_{head})\,\pi\varepsilon R^2 \frac{2J_1(qR'(\varphi)sin\theta)}{qR'(\varphi)sin\theta} \frac{sin(qH_{tail}\,cos\theta/2)}{q\,cos\theta/2} +$$

$$+(\rho_{head} - \rho_{belt})\,\pi\varepsilon R^2 \frac{2J_1(qR'(\varphi)sin\theta)}{qR'(\varphi)sin\theta} \frac{sin(q(H_{tail}+2H_{head})cos\theta/2)}{q\,cos\theta/2} + \quad [6]$$

$$+(\rho_{belt} - \rho_{aver})\,\pi\varepsilon\Delta R(2R+\Delta R) \times$$

$$\times \frac{2J_1(q(R'(\varphi)+\Delta R)sin\theta)}{q(R'(\varphi)+\Delta R)sin\theta} \frac{sin(q(H_{tail}+2H_{head})cos\theta/2)}{q\,cos\theta/2},$$

where the effective radius $R'(\varphi)$ is equal to

$$R'(\varphi) = \frac{R}{\sqrt{2}}\sqrt{(1+\varepsilon^2)+(1-\varepsilon^2)\,cos\varphi} \quad [7]$$

and the average scattering length density (SLD) of the solution is equal to

$$\rho_{aver} = (1-f)\,\rho_{solvent} +$$

$$+f\frac{\pi\varepsilon R^2\rho_{tail}H_{tail} + 2\pi\varepsilon R^2\rho_{head}H_{head} + \pi\varepsilon\Delta R(2R+\Delta R)(H_{tail}+2H_{head})}{\pi\varepsilon(R+\Delta R)^2(H_{tail}+2H_{head})}, \quad [8]$$

where f is the volume fraction of the bicelles/ribbons. Usually, when parameter f is small enough, the following approximate equality holds: $\rho_{aver} \approx \rho_{solvent}$. However, in our case, the volume fraction is in a range of 5.6-14%, which is not negligible. Theoretical $P(q)$ for the bicelles and the ribbons (see Fig. 7) are special cases of equations [5-8] corresponding to conditions $\varepsilon \approx 1$ (for Model 1) and $T_{shell} = H_{head} = \Delta R$, $L = H_{tail}$, and $\rho_{shell} \approx \rho_{belt} \approx \rho_{head}$ (for Model 2), respectively.

Murugova, T.N., Ivankov, O.I., Ryzhykau, Y.L. et al. Mechanisms of membrane protein crystallization in 'bicelles'. Sci Rep 12, 11109 (2022).

Structural evolution of crystallization matrix

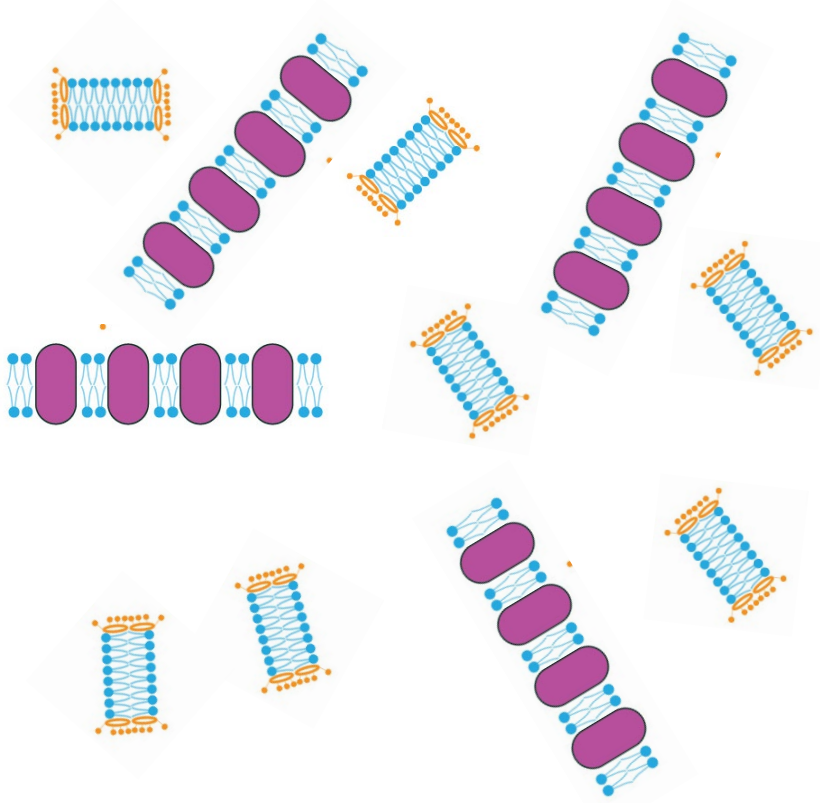

D_{bic} = 100 Å, T_{bic} = 40Å

Murugova, T.N., Ivankov, O.I., Ryzhykau, Y.L. et al. Mechanisms of membrane protein crystallization in ‘bicelles’. Sci Rep 12, 11109 (2022).

Structural evolution of crystallization matrix

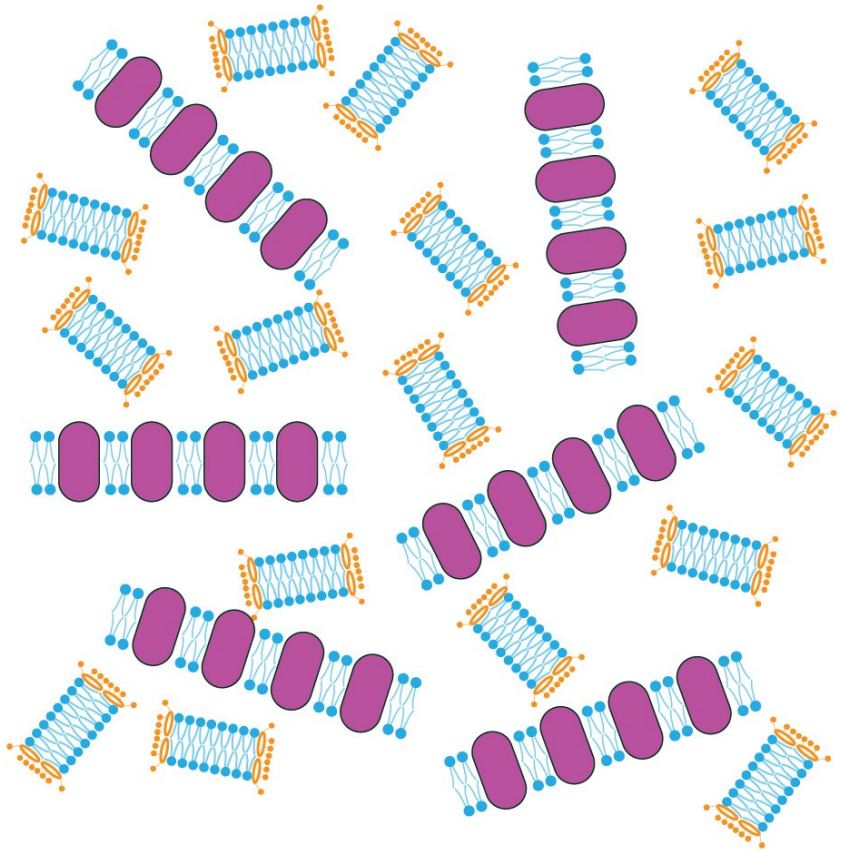

D_{bic} = 100 Å, T_{bic} = 40Å

Murugova, T.N., Ivankov, O.I., Ryzhykau, Y.L. et al. Mechanisms of membrane protein crystallization in ‘bicelles’. Sci Rep 12, 11109 (2022).

Structural evolution of crystallization matrix

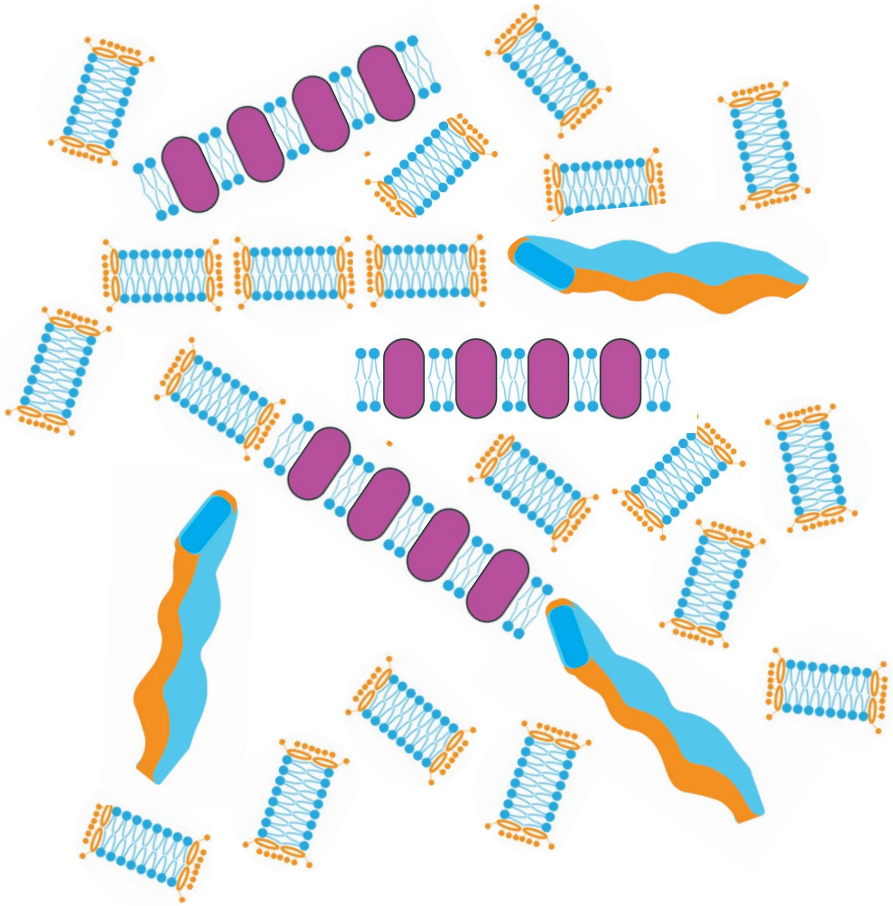

L_{rib} = 300-500 Å, T_{rib} = 60-70 Å , T_{rib} = 110-120 Å

Murugova, T.N., Ivankov, O.I., Ryzhykau, Y.L. et al. Mechanisms of membrane protein crystallization in ‘bicelles’. Sci Rep 12, 11109 (2022).

Structural evolution of crystallization matrix

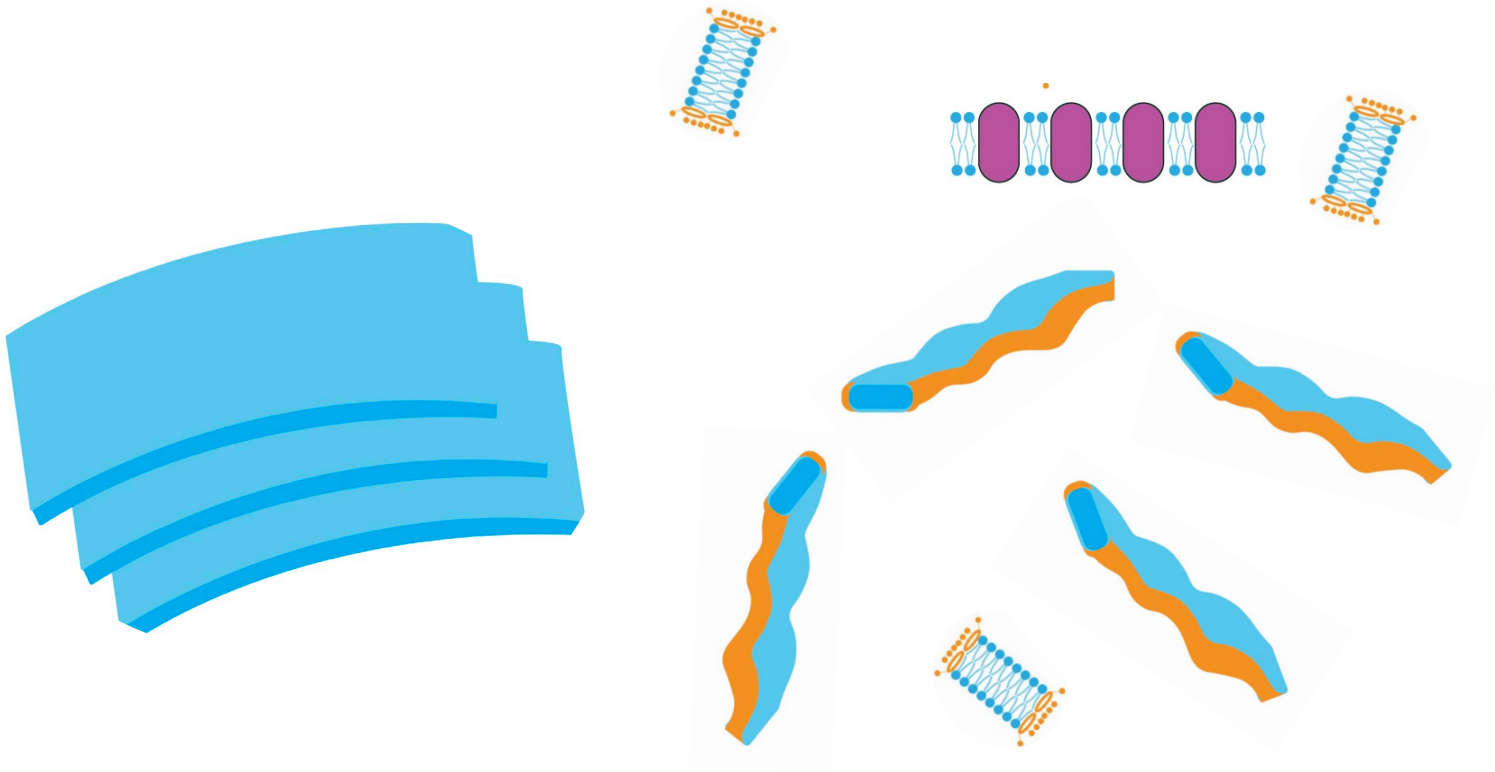

d = 73 Å

Murugova, T.N., Ivankov, O.I., Ryzhykau, Y.L. et al. Mechanisms of membrane protein crystallization in ‘bicelles’. Sci Rep 12, 11109 (2022).

Structural evolution of crystallization matrix

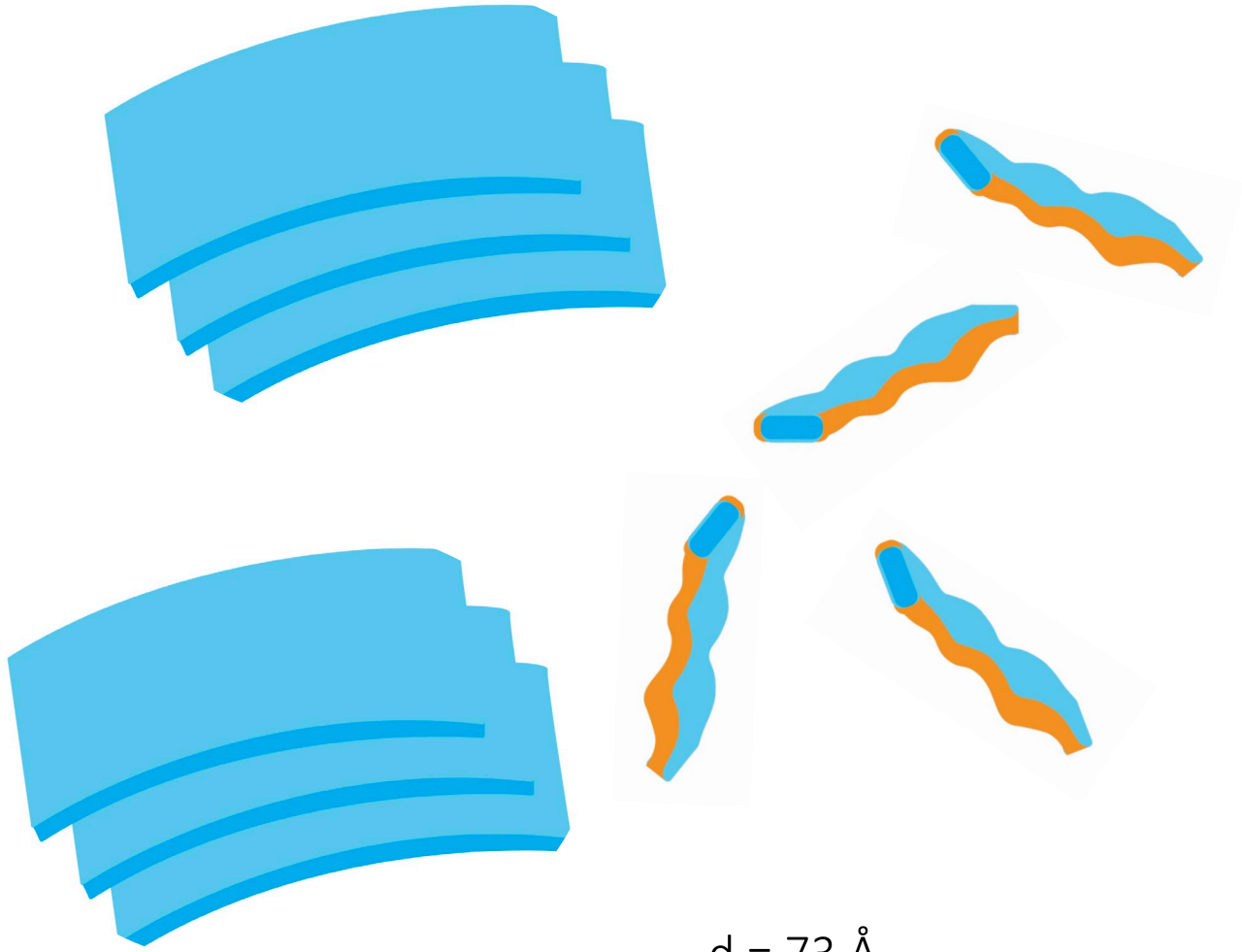

d = 73 Å

Murugova, T.N., Ivankov, O.I., Ryzhykau, Y.L. et al. Mechanisms of membrane protein crystallization in ‘bicelles’. Sci Rep 12, 11109 (2022).

Structural evolution of crystallization matrix

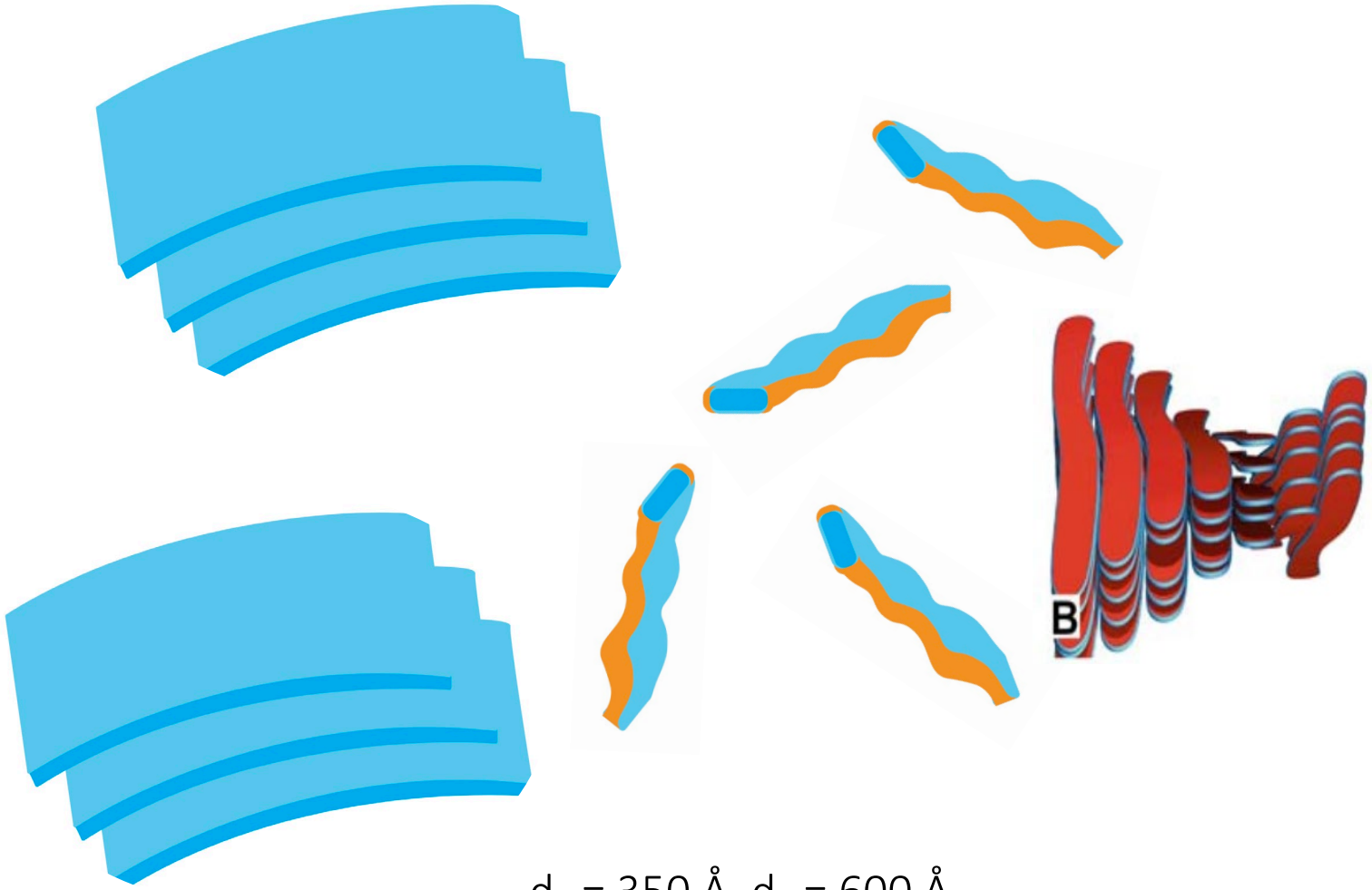

d_1 = 350 Å, d_1 = 600 Å

Murugova, T.N., Ivankov, O.I., Ryzhykau, Y.L. et al. Mechanisms of membrane protein crystallization in ‘bicelles’. Sci Rep 12, 11109 (2022).

Structural evolution of crystallization matrix

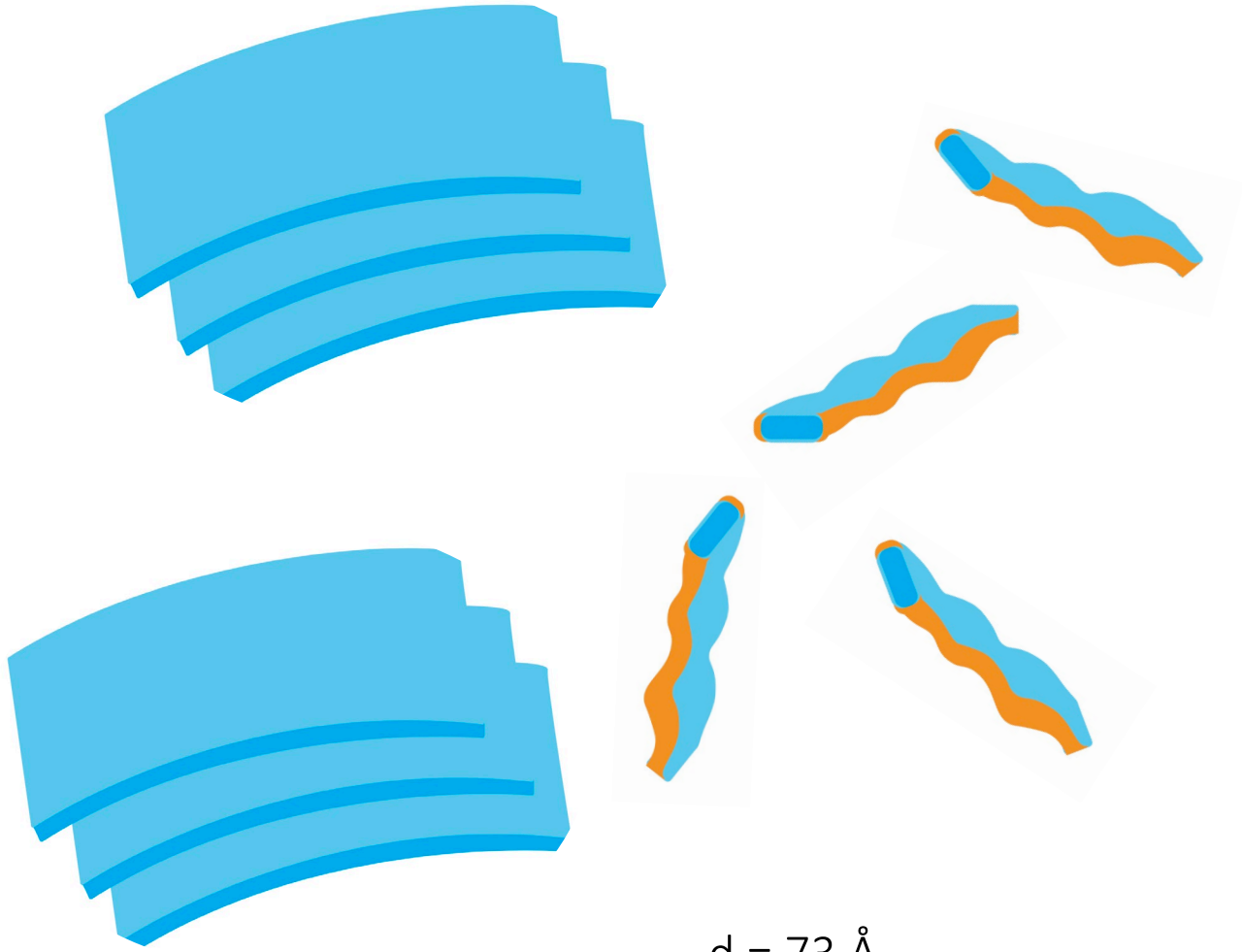

d = 73 Å

Murugova, T.N., Ivankov, O.I., Ryzhykau, Y.L. et al. Mechanisms of membrane protein crystallization in ‘bicelles’. Sci Rep 12, 11109 (2022).

Structural evolution of crystallization matrix

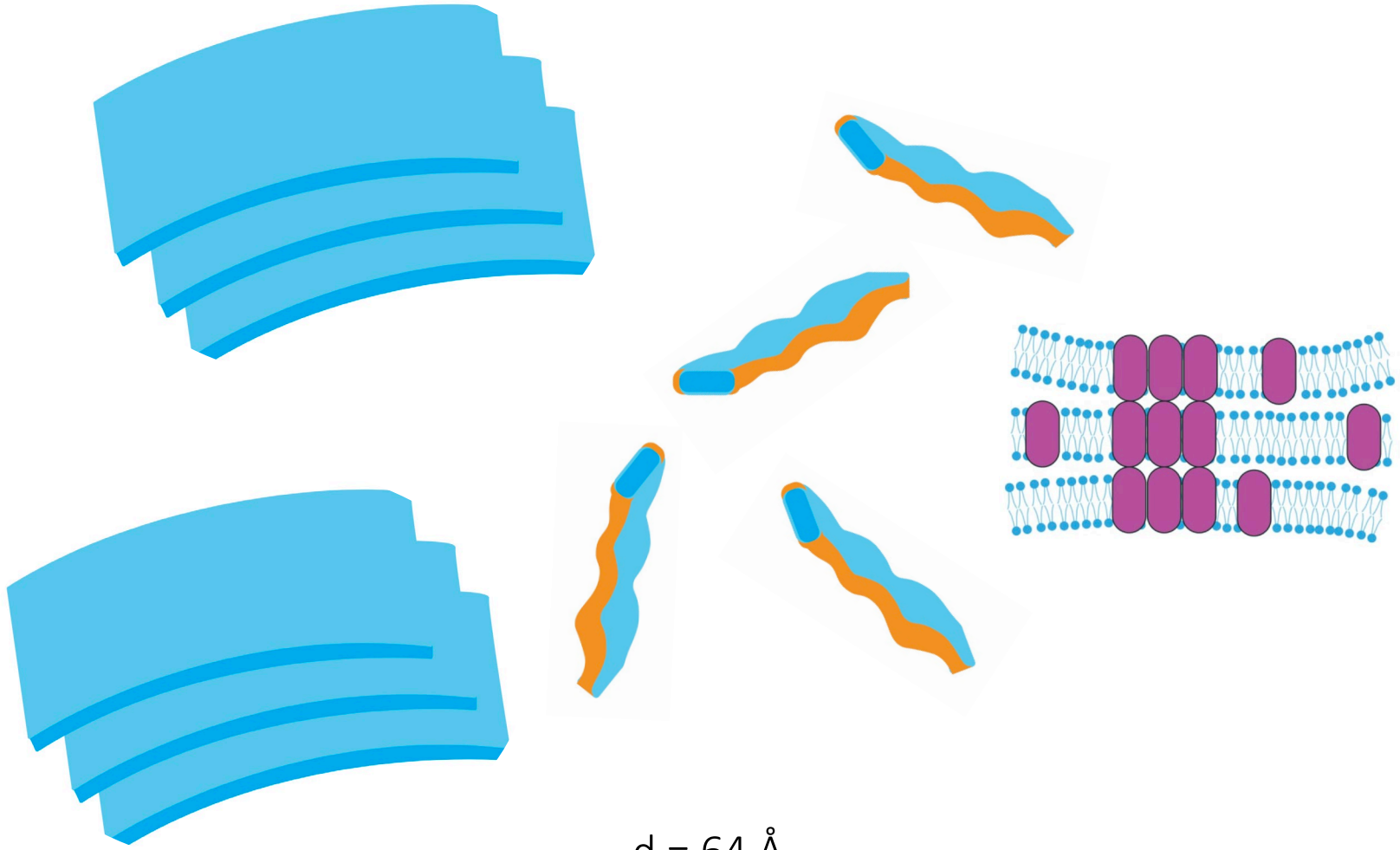

d = 64 Å

Murugova, T.N., Ivankov, O.I., Ryzhykau, Y.L. et al. Mechanisms of membrane protein crystallization in ‘bicelles’. Sci Rep 12, 11109 (2022).

Structural evolution of crystallization matrix

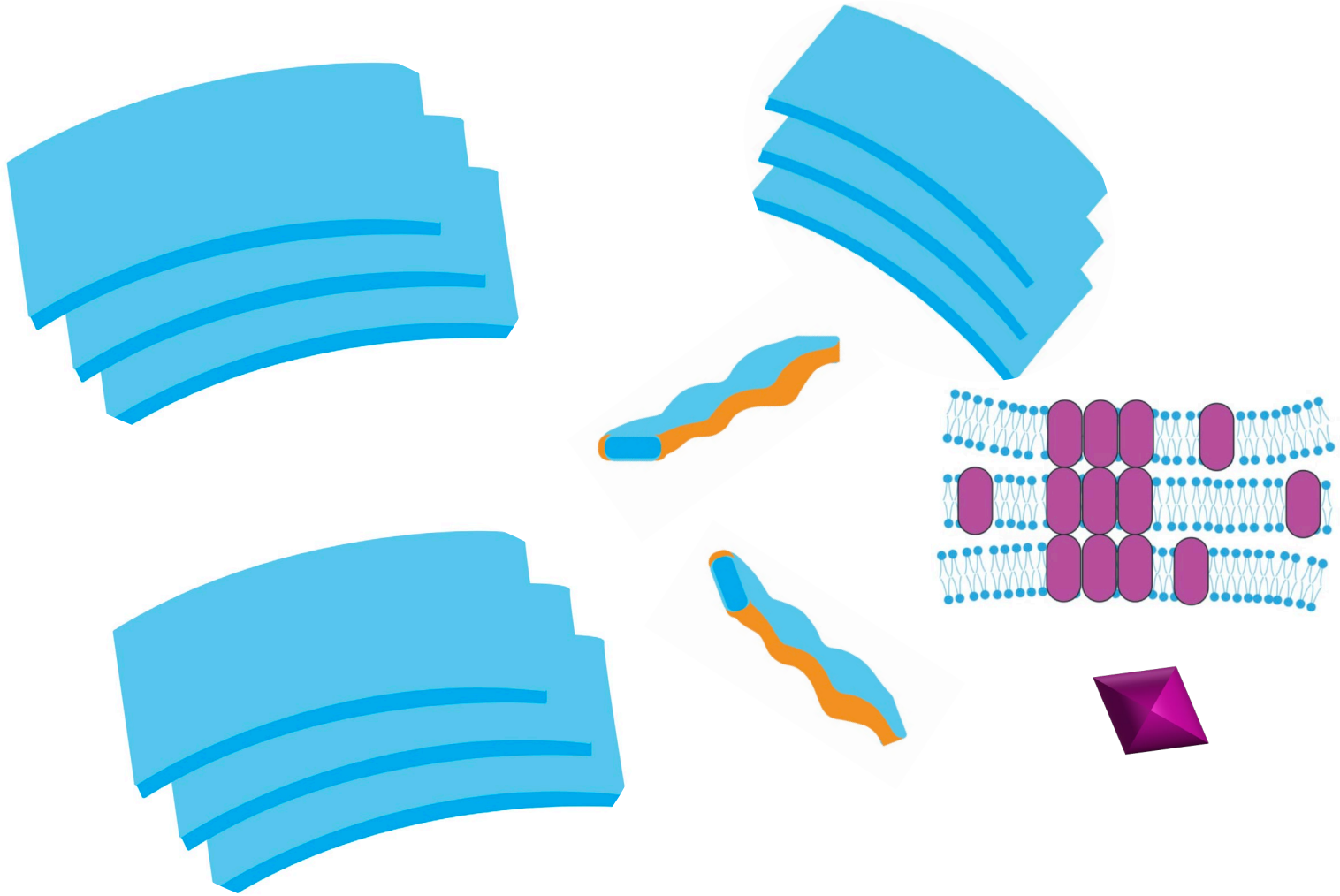

Murugova, T.N., Ivankov, O.I., Ryzhykau, Y.L. et al. Mechanisms of membrane protein crystallization in ‘bicelles’. Sci Rep 12, 11109 (2022).

Structural evolution of crystallization matrix

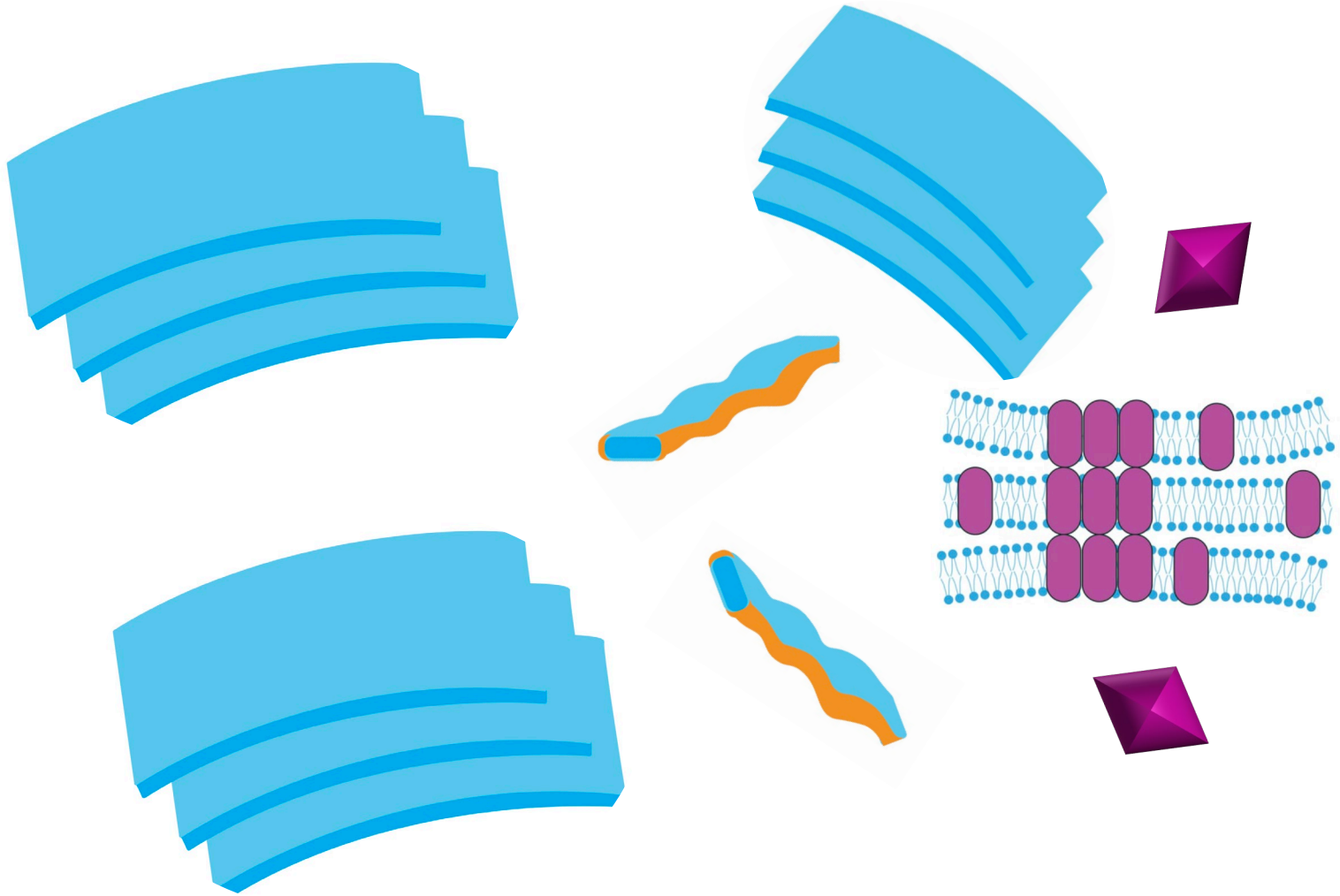

Murugova, T.N., Ivankov, O.I., Ryzhykau, Y.L. et al. Mechanisms of membrane protein crystallization in ‘bicelles’. Sci Rep 12, 11109 (2022).

Structural evolution of crystallization matrix

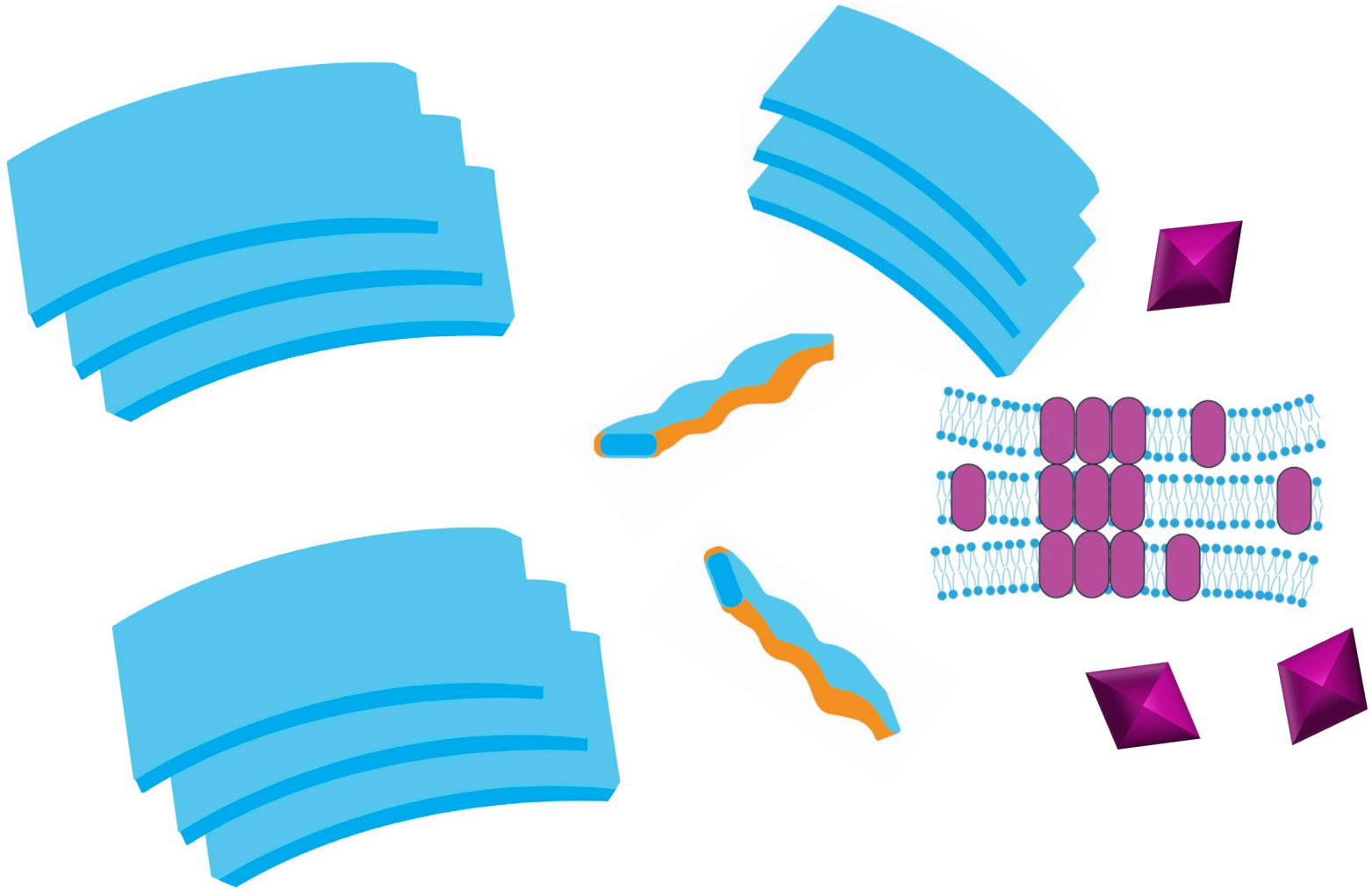

Murugova, T.N., Ivankov, O.I., Ryzhykau, Y.L. et al. Mechanisms of membrane protein crystallization in ‘bicelles’. Sci Rep 12, 11109 (2022).

Structural evolution of crystallization matrix

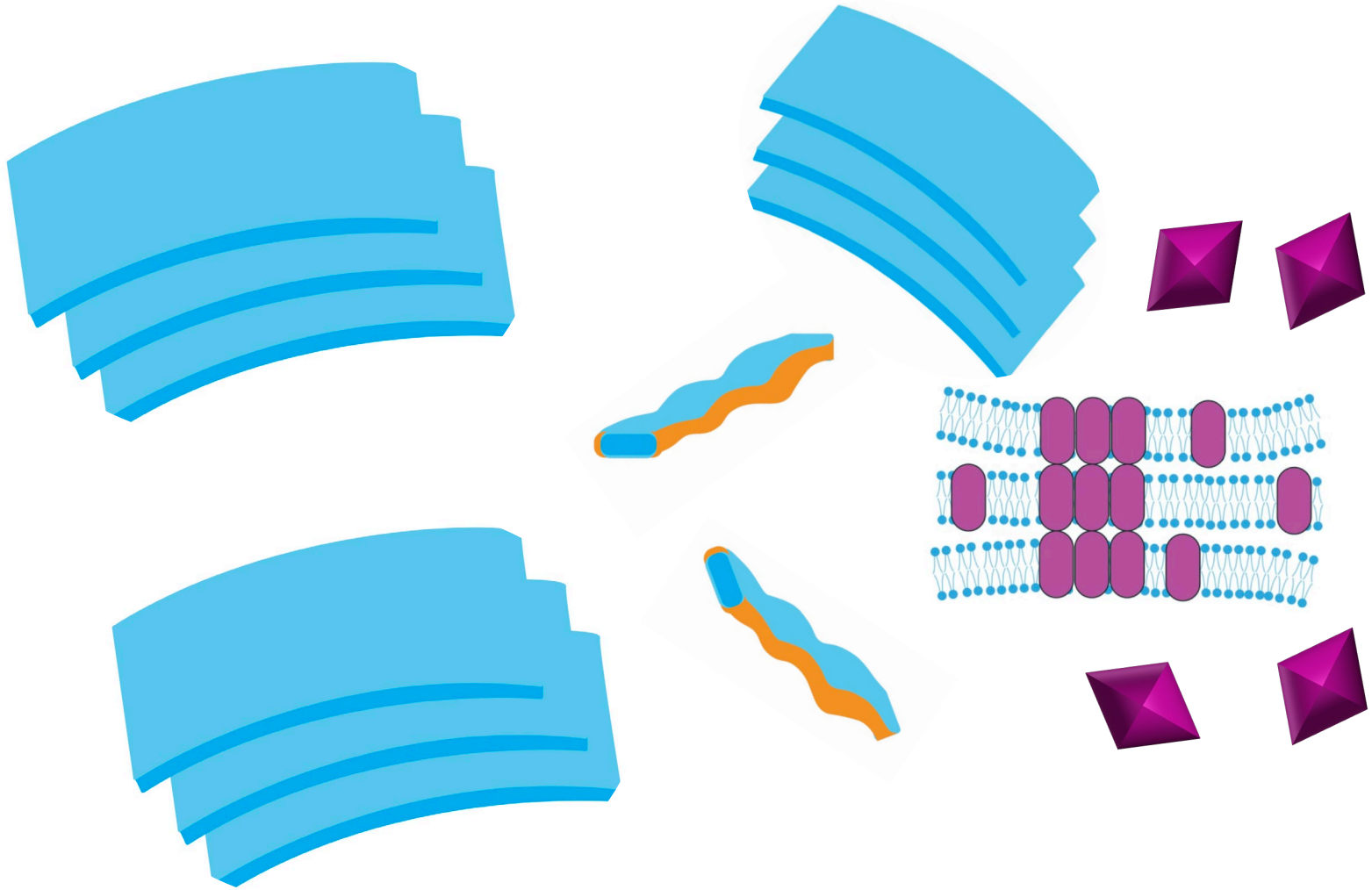

Murugova, T.N., Ivankov, O.I., Ryzhykau, Y.L. et al. Mechanisms of membrane protein crystallization in ‘bicelles’. Sci Rep 12, 11109 (2022).

Summary

- Crystals grow not in bicelles, but in the jelly-like lipidic system containing elongated ribbons and multilamellar phase.
- The bicelles are only the initial state of crystallization matrix.
- Upon crystals formation the local multilamellar phase appears that surrounds the crystals and is critical for crystal growth.
- We hope that our information will support rational design of crystallization

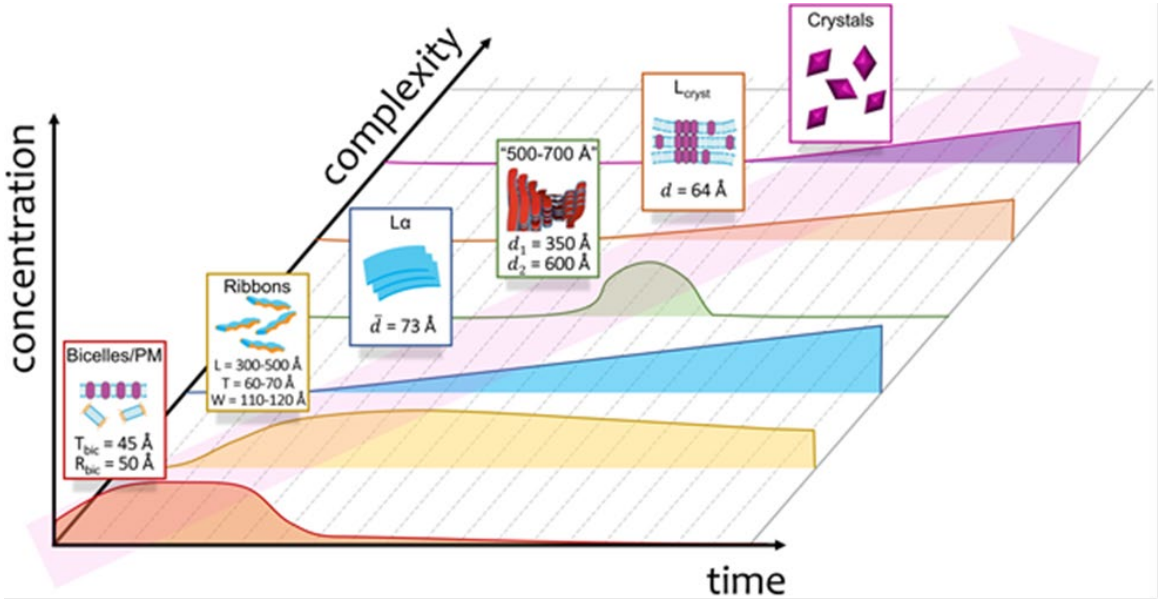

JINR participants, SANS group

Dr. Gordeliy V.I.

Dr. Ivankov A.I.

Dr. Kuklin A.I.

Dr. Murugova T.N.

Dr. Rogachev A.V.

Dr. Ryzhykau Yu.L.

Dr. Soloviov D.V.

Dr. Vlasov A.V.

K. V. Kovalev (EMBL, Hamburg)

D. V. Skachkova (previously FLNP JINR)

A. Round (previously ESRF)

C. Baeken (Forschungszentrum Jülich)

A. V. Ishchenko (previously Forschungszentrum Jülich)

O. A. Volkov (previously Forschungszentrum Jülich)

Thank you for your attention!

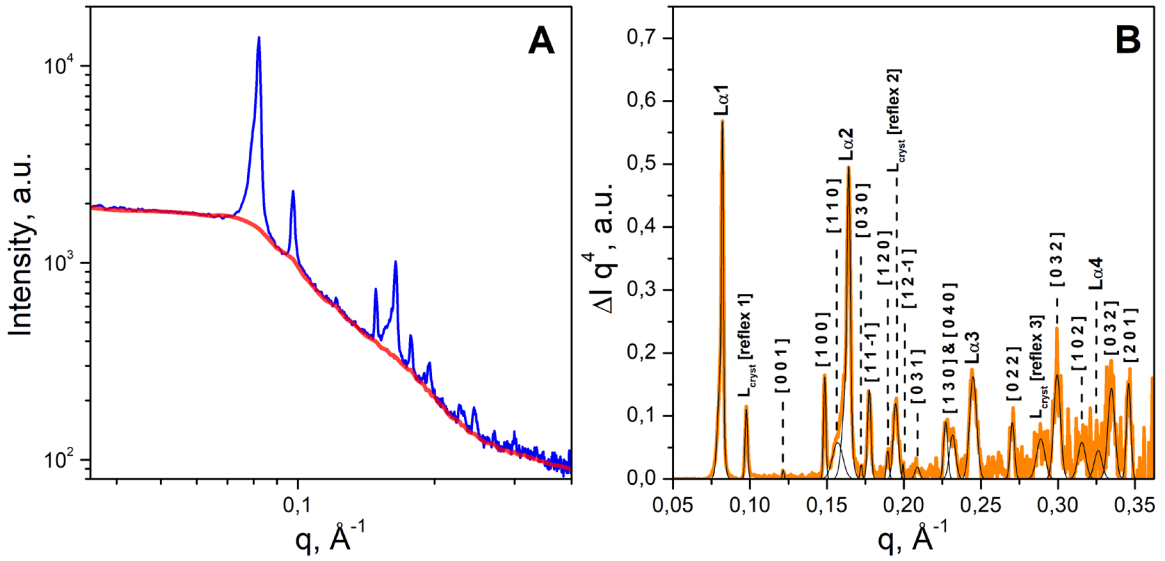

Figure 5. SAXS data from the crystallization matrix after crystal formation (BM29, ESRF). (**A**) – The SAXS curve for the crystallization matrix with crystals (blue curve) and the corresponding baseline (red curve). (B) – The SAXS curve from the crystallization matrix after baseline subtraction (orange). Intensity is multiplied by q^4 for better observation of the wide-angle peaks. The Gaussian approximations of the peaks are represented in black. The Miller indexes (for BR crystals) and the reflex numbers (for the lipidic multilayers Lα or L_{cryst}) are marked above the corresponding peaks (for more details, see Supplementary Table S2).

Murugova, T.N., Ivankov, O.I., Ryzhykau, Y.L. et al. Mechanisms of membrane protein crystallization in 'bicelles'. Sci Rep 12, 11109 (2022).

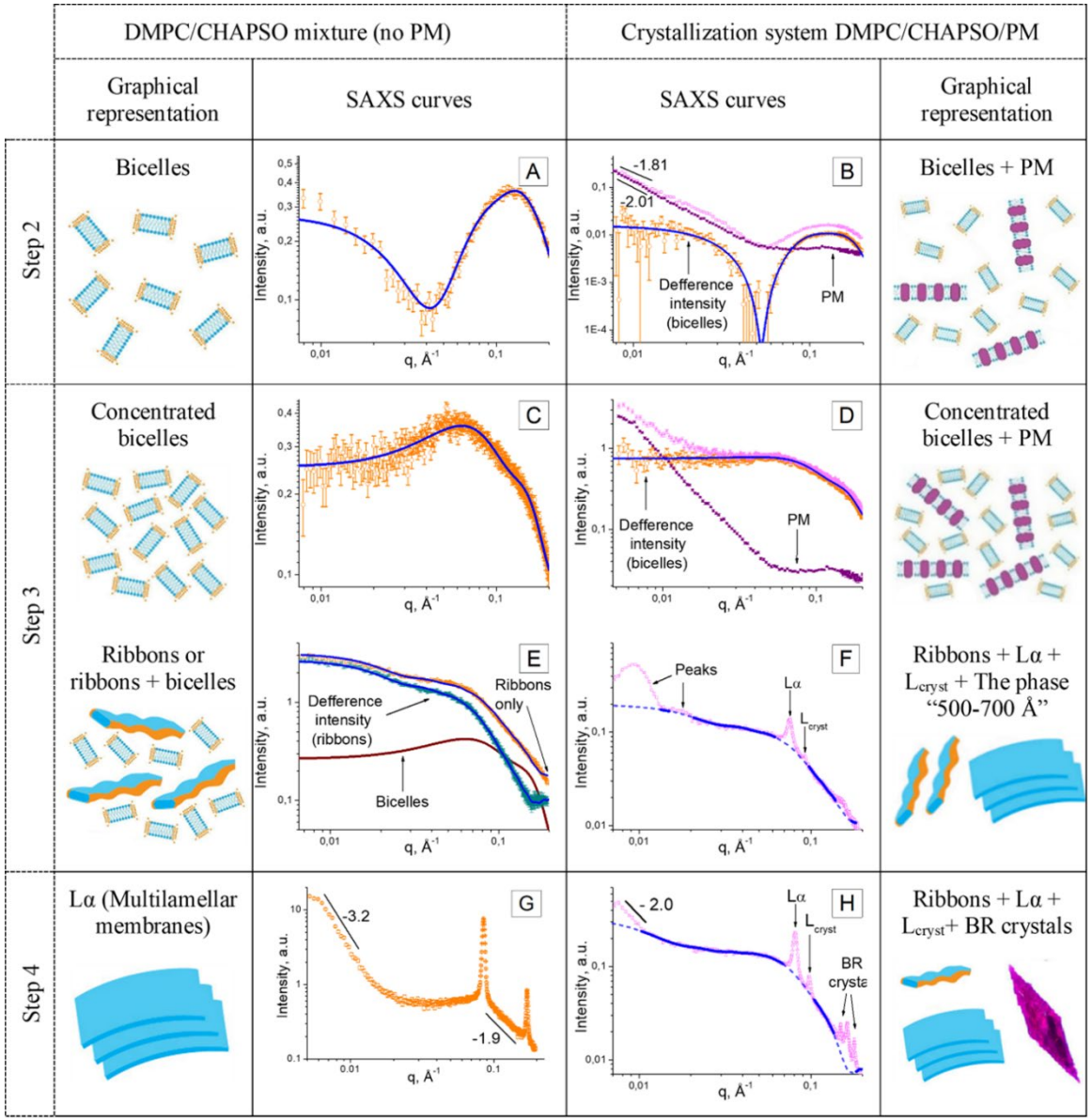

Evolution of the crystallization matrix during the crystallization process. The SAXS curves for the pure DMPC/CHAPSO mixture without PM (left) and the crystallization system DMPC/CHAPSO/PM (right). Experimental data for crystallization system with and without PM are shown as light purple and orange hollow circles, correspondingly. SAXS curves for PM are shown as dark purple squares. The approximations by form-factors of the bicelles and the ribbons are shown as blue lines. The graphical representations of the structural organizations of the crystallization matrix are shown adjacent to the corresponding SAXS curves.

Murugova, T.N., Ivankov, O.I., Ryzhykau, Y.L. et al. Mechanisms of membrane protein crystallization in 'bicelles'. Sci Rep 12, 11109 (2022).

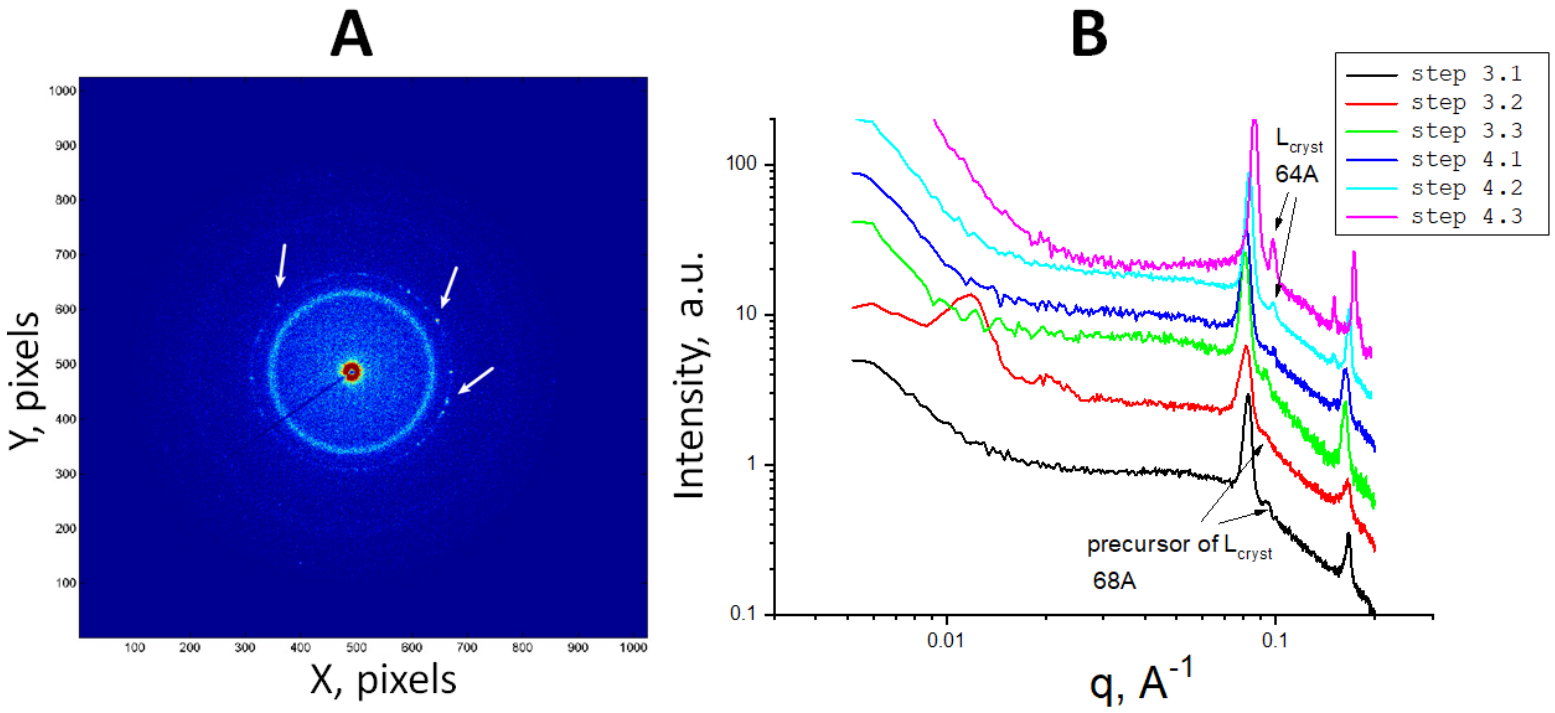

Behavior of the peak for the local lamellar phase L_{cryst}. (**A**) – 2D pattern for the sample containing the BR crystals (corresponds to 1D curve step 4.3 in Figure 3). The reflections corresponding to the local lamellar phase L_{cryst} are shown by white arrows. The scattering ring belongs to the multilamellar phase Lα with a spacing of about 84 Å. (**B**) – Behavior of the peak for the local lamellar phase L_{cryst} on the 1D curves. All the SAXS curves belong to different time points of the same sample. The crystallization conditions are the same as for the sample in Figure 3.

Murugova, T.N., Ivankov, O.I., Ryzhykau, Y.L. et al. Mechanisms of membrane protein crystallization in 'bicelles'. Sci Rep 12, 11109 (2022).

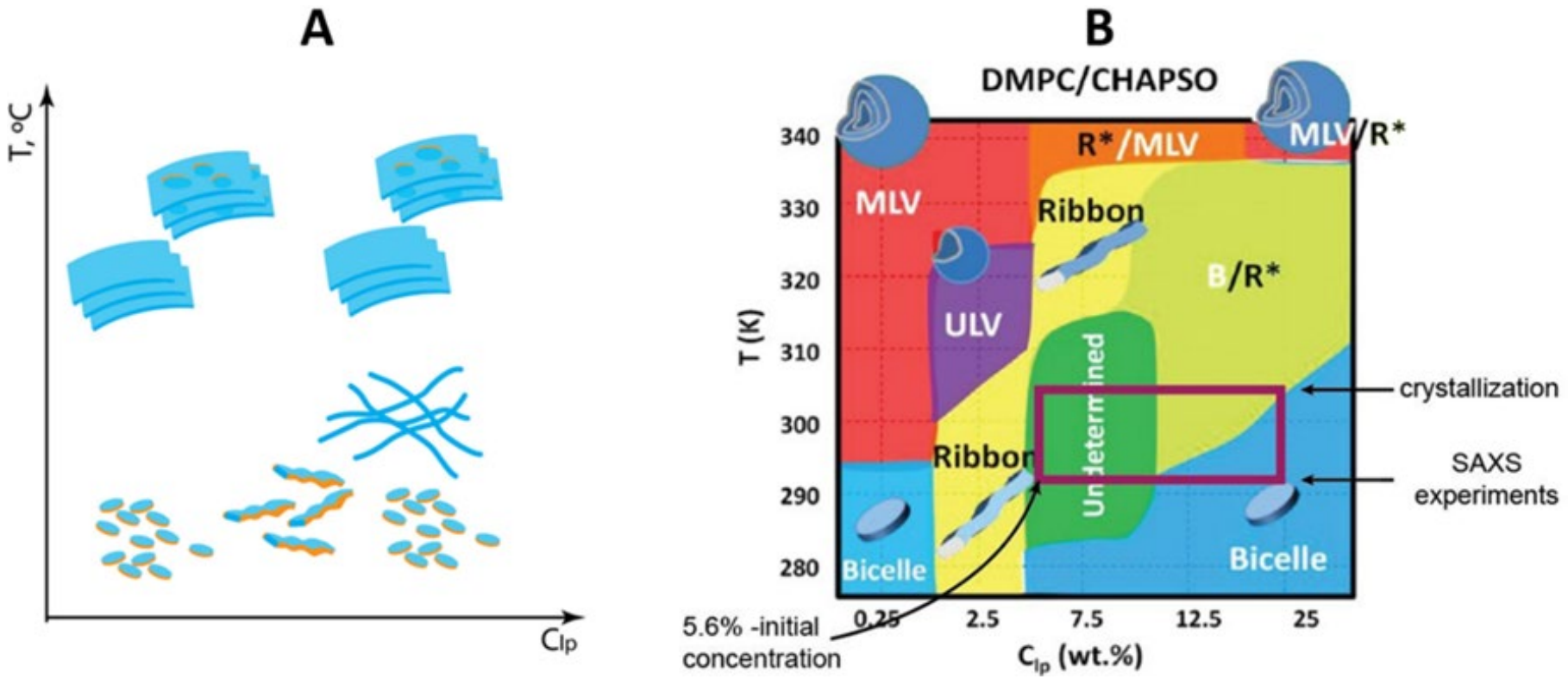

Phase diagram for the DMPC/CHAPSO bicellar system.
(A) – Schematic phase diagram showing structural behavior of the bicellar systems. (B) – The phase diagram for the DMPC/CHAPSO mixture at molar ratio Q = 3. The purple rectangle highlights the conditions used in this work.
Panel B was adapted with permission from (19). Copyright (2013) American Chemical Society.

Murugova, T.N., Ivankov, O.I., Ryzhykau, Y.L. et al. Mechanisms of membrane protein crystallization in ‘bicelles’. Sci Rep 12, 11109 (2022).

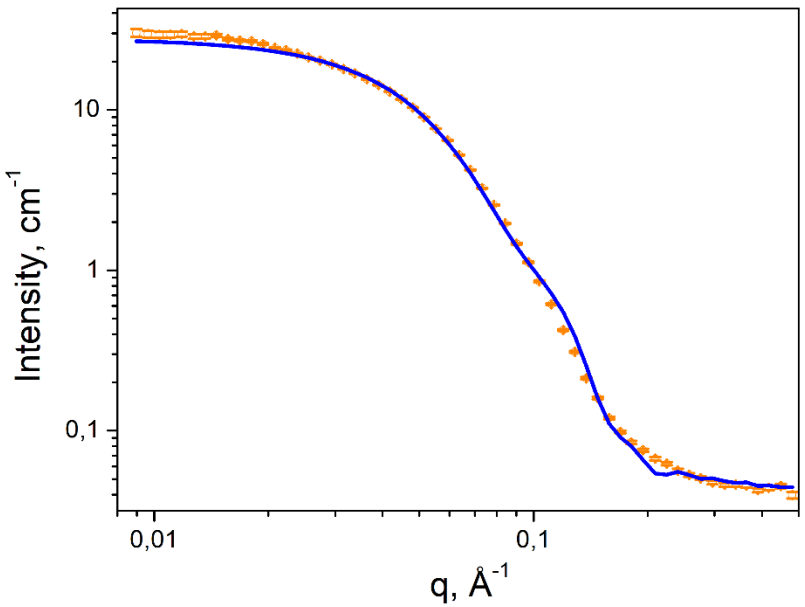

Fig. S3. SANS data for the bicelles. Experimental SANS data for bicelles in D2O–buffer (orange hollow circles) and corresponding fit by the form-factor of bicelles (blue curve, see fit parameters in Table 2).

Murugova, T.N., Ivankov, O.I., Ryzhykau, Y.L. et al. Mechanisms of membrane protein crystallization in ‘bicelles’. Sci Rep 12, 11109 (2022).

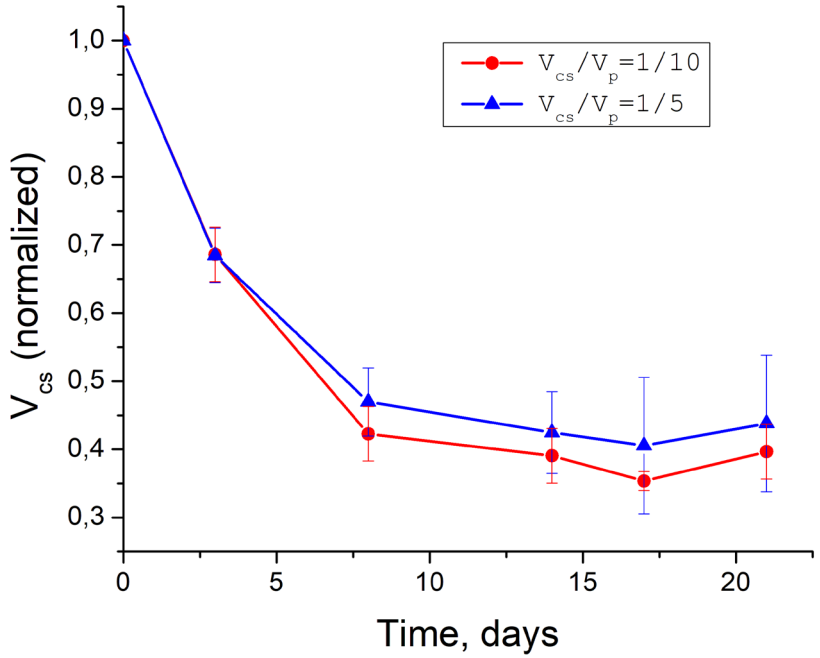

Fig. S4. Changes in the volume of the crystallization system during the evaporation process. The observed height of the crystallization system in a capillary during the crystallization process. The presented values are averaged over 4-5 capillaries and normalized on the height of the system on the first day of the pouring system in a capillary. Vcs/Vp – volume ratio of the crystallization system and the precipitant in the capillary (Vcs and Vp mean volume of the crystallization system and the precipitant, correspondingly).

Murugova, T.N., Ivankov, O.I., Ryzhykau, Y.L. et al. Mechanisms of membrane protein crystallization in ‘bicelles’. Sci Rep 12, 11109 (2022).

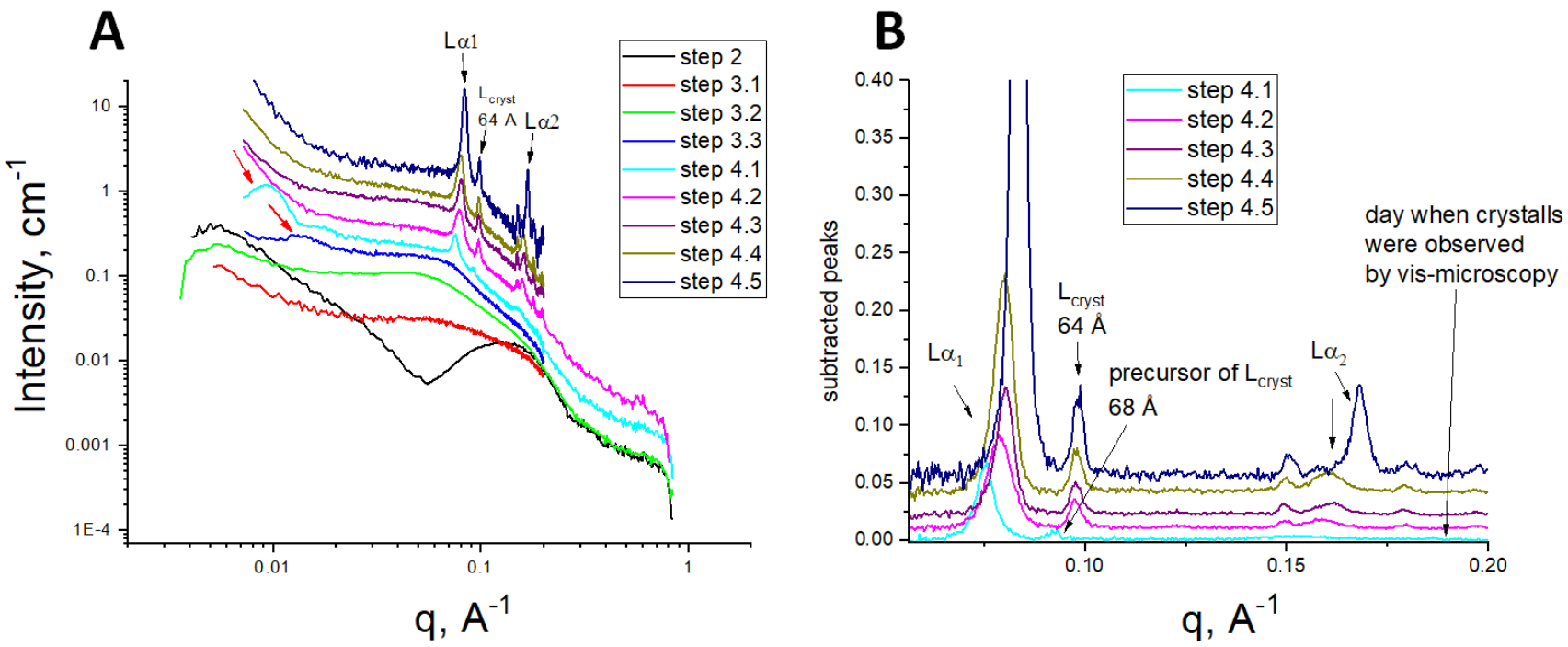

Figure 3. Transformation of the SAXS curves for the crystallization system during the different steps of the crystallization process. (**A**) – The SAXS curves related to different steps of the crystallization process. The red arrows in the small angle region indicate the interference peaks from the lipid/detergent smectic phase (curve designations are given in the legend; steps numbering is described in Figure 1). (**B**) – The peaks extracted from the SAXS curves (part A) by subtraction of the baseline. The curves are scaled to separate them vertically for better visualization. The black arrows "$L\alpha_1$" and "$L\alpha_2$" (shown in both A and B) indicate the lamellar peaks of the first and second order; the other black arrow "L_{cryst} 64 Å" indicates the peak from the local lamellar phase bonded with the protein surface, the spacing of this L_{cryst} is 64 Å. The arrow "68 Å" indicates the precursor of the L_{cryst} phase.